

Frequency-domain nonlinearity analysis of noise from a high-performance jet aircraft

Kent L. Gee, Kyle G. Miller, Brent O. Reichman, and Alan T. Wall

Citation: *Proc. Mtgs. Acoust.* **34**, 045027 (2018); doi: 10.1121/2.0000899

View online: <https://doi.org/10.1121/2.0000899>

View Table of Contents: <https://asa.scitation.org/toc/pma/34/1>

Published by the [Acoustical Society of America](#)

ARTICLES YOU MAY BE INTERESTED IN

[Nonlinear propagation of shaped supersonic signatures through turbulence](#)

Proceedings of Meetings on Acoustics **34**, 045011 (2018); <https://doi.org/10.1121/2.0000872>

[A measurement system for the study of nonlinear propagation through arrays of scatterers](#)

Proceedings of Meetings on Acoustics **34**, 045026 (2018); <https://doi.org/10.1121/2.0000889>

[Turbulent flow due to the interaction of two mutually perpendicular crossed turbulent streaming jets in water](#)

Proceedings of Meetings on Acoustics **34**, 045022 (2018); <https://doi.org/10.1121/2.0000884>

[Feasibility study of using acoustic methods for regionalizing an impact force acting on a structure](#)

Proceedings of Meetings on Acoustics **33**, 065002 (2018); <https://doi.org/10.1121/2.0000924>

[Towards higher energy density processes in sonoluminescing bubbles](#)

Proceedings of Meetings on Acoustics **34**, 045017 (2018); <https://doi.org/10.1121/2.0000869>

[Characterization of wave fields using transient motion of microspheres under acoustic radiation force](#)

Proceedings of Meetings on Acoustics **34**, 030003 (2018); <https://doi.org/10.1121/2.0000871>



21st International Symposium on Nonlinear Acoustics



Physical Acoustics: S8-3

Frequency-domain nonlinearity analysis of noise from a high-performance jet aircraft

Kent L. Gee

Department of Physics and Astronomy, Brigham Young University, Provo, UT, 84602; kentgee@byu.edu

Kyle G. Miller and Brent O. Reichman

Brigham Young University, Provo, UT, 84602; kglennmiller@gmail.com; brent.reichman@gmail.com

Alan T. Wall

Air Force Research Laboratory, Wright-Patterson Air Force Base, OH; alan.wall.4@us.af.mil

Characterization of far-field jet noise spectral evolution can be performed locally with a single microphone measurement using a gain factor that stems from the ensemble-averaged, frequency-domain version of the generalized Burgers equation. The factor quantifies the nonlinear change in the sound pressure level spectrum over distance [B. O. Reichman et al., *J. Acoust. Soc. Am.* 139, 2505-2513 (2016)]. Here, noise waveforms from a high-performance military jet aircraft are characterized with this gain factor and compared to propagation losses from geometric spreading and atmospheric absorption. Far-field results show that the high-frequency nonlinear gains at high frequencies tend to balance the absorption losses, thus establishing the characteristic spectral slope present in shock-containing noise. Differences as a function of angle, distance, and engine condition are explored.



1. INTRODUCTION

Noise propagation from high-performance tactical jet aircraft has been previously shown to be nonlinear.^{1,2} Waveform steepening and shock formation result in greater high-frequency sound levels in the far field, causing an apparent reduction in atmospheric absorption. The importance of nonlinearity relative to absorption can be quantified via a nonlinearity analysis³ based on the ensemble-averaged, frequency-domain generalized Burgers equation (GBE). It has been performed recently for laboratory-scale jet noise,⁴ but here is applied to the relative roles of nonlinearity and atmospheric absorption for measurements of an F-35A aircraft.

Morfeý and Howell⁵ found that an ensemble-averaged form of the GBE included a spectral quantity that could be used as a nonlinearity indicator. The Morfeý and Howell-derived Q/S spectrum is defined for a pressure waveform, $p(t)$, as

$$\frac{Q}{S} = \frac{Q_{pp^2}}{p_{\text{rms}}S_{pp}} = \frac{\text{Im}\{E[\mathcal{F}^*\{p(t)\}\mathcal{F}\{p^2(t)\}]\}}{p_{\text{rms}}S_{pp}}, \quad (1)$$

where Q_{pp^2} is the imaginary part of the cross-spectral density (or quadspectral density) between the pressure and pressure-squared waveforms, p_{rms} is the root-mean-square pressure, and S_{pp} is the autospectral density. Also, E denotes expectation value and \mathcal{F} denotes a Fourier transform. Because Q/S involves the quadspectral density between pressure and squared pressure, it reveals quadratic phase coupling across frequencies.⁹ The Q/S indicator has been variously applied to military aircraft noise,^{6,7} laboratory jet noise,^{8,9} rocket noise,¹⁰ and plane-wave tube data.⁹

While the Q/S indicator has been useful for qualitative nonlinearity analyses, a quantitative interpretation requires an understanding of its magnitude relative to other propagation mechanisms. To this end, the Q/S metric is used here in conjunction with GBE terms that account for spherical spreading and atmospheric absorption. An ensemble-averaged version of the frequency-domain GBE yields an expression³ for the change in sound pressure level (SPL) over distance, r :

$$\frac{\partial L_p}{\partial r} = -\eta \times \left(\frac{2}{r} + 2\alpha + \frac{\omega\beta p_{\text{rms}} Q}{\rho_0 c_0^3 S} \right) \equiv \nu_S + \nu_\alpha + \nu_N \equiv \nu, \quad (2)$$

where L_p is the sound pressure level spectrum (in decibels), $\eta \equiv 10 \log_{10}(e) \approx 4.34$, α is the frequency-dependent linear absorption coefficient, ω is radian frequency, β is the coefficient of nonlinearity, and ρ_0 and c_0 are the ambient density and sound speed, respectively. In addition, the indicators listed on the right-hand side of Eq. (2), by observation, are defined as

$$\nu_S \equiv -\eta \times \frac{2}{r}, \quad \nu_\alpha \equiv -\eta \times 2\alpha, \quad \nu_N \equiv -\eta \times \frac{\omega\beta p_{\text{rms}} Q}{\rho_0 c_0^3 S}. \quad (3)$$

Equation (3) gives expressions for the rate of change in level spectrum over distance due to spherical spreading, absorption, and nonlinearity, respectively. When calculated and compared in conjunction, the three indicators quantitatively relate three separate effects, with each indicator carrying explicit physical meaning. Positive values of the quantities in Eq. (3) indicate growth and negative values indicate decay. Analytical studies^{3,11} of these indicators for initially sinusoidal waves in thermoviscous media show that prior to shock formation, ν_N and $\nu_\alpha + \nu_N$ are both positive for high frequencies, whereas after shock formation and into the old-age region, $\nu_\alpha + \nu_N$ is negative while ν_N remains positive. Thus, when combined they result in a reduced apparent atmospheric absorption rate.

2. MEASUREMENT

The F-35A run-up measurements analyzed here comprised 90 locations along arcs with radii of 19.1, 28.6, 38.1, 76.2, 152, and 305 m (63, 94, 125, 250, 500, and 1000 ft), relative to an origin located 6.6 m behind the engine nozzle exit. Microphones at each radius ranged from 0° to 160° relative to the engine

inlet, with heights ranging from 1.5 to 9.1 m. Waveform data were sampled at 204.8 kHz at all microphones except at 305 m, where data were sampled at 96 kHz from 0° to 80° and at 51.2 kHz from 90° to 160°. Temperature during the early-morning measurements varied between 19.4°C and 23.1°C, and the relative humidity varied between 37.6% and 45.7%. The average wind speed was 1.7 m/s. This paper focuses on engine conditions of 50%, 75% and 130% (minimum afterburner) engine thrust request. See Ref. 12 for more information on the experimental setup, conditions, and analyses.

3. NONLINEARITY ANALYSIS

Shown in Fig. 1 is a map of the overall sound pressure level (OASPL) for 130% ETR, with a regularized cubic spline interpolation between the marked measurement positions and with the aircraft drawn to scale. The peak radiation angular range spans approximately 120 – 135°, with levels at 19 m exceeding 143 dB. At 305 m, levels at these angles are greater than 120 dB. In the forward direction, the OASPL is approximately 10 dB lower, but the tendency toward linearity in the forward direction is partially offset by a peak frequency that is 3-5 times greater than in the aft direction. Figure 1 also shows the one-third-octave (OTO) spectra along the 135° radial. These spectra reveal expected geometric (near-spherical) spreading, a near complete lack of high-frequency absorption effect, given the $\sim f^{-2}$ power-law slope only begins to roll off slightly by 305 m, and some irregularities due to both ground reflections (400 Hz – 1000 Hz) and microphone mounting (>2000 Hz). These irregularities, which represent amplitude and phase changes due to multipath interference, can cause oscillations in the calculated ν_N , which is shown for 135° and 130% ETR in the right panel of Fig. 1. However, despite the resultant noisiness (that unfortunately extends to 20 kHz for the 38 m (125 ft) case), the clear trend in the OTO ν_N is a tendency to increasingly greater values at high frequencies. The ν_N analysis shows that, at 20 kHz, the levels at 76 m and beyond are increasing by ~ 0.6 dB/m due to nonlinearity. The nearly constant roll-off in the OTO spectrum with distance further suggests that the nonlinearity and the absorption are approximately balanced.

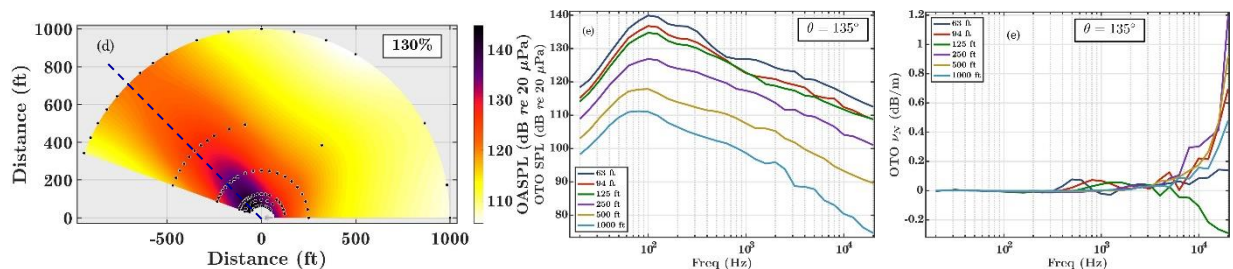


Figure 1. Left: F-35A OASPL for 130% ETR. Middle: One-third octave spectra along the 135° radial for a 130% ETR run-up, near the maximum radiation direction. Right: OTO ν_N calculation for the same run-up.

Figure 2 displays spatial maps of the OTO ν_N at 100 Hz and 10 kHz, for three different engine conditions: low power (50% ETR), intermediate power (75% ETR), and minimum afterburner (130% ETR). The lower frequency was selected because it is near the peak-frequency region of the spectrum in the maximum radiation direction. The higher frequency, on the other hand, shows characteristic behavior at frequencies important to shock formation and nonlinear spectral gains. At 100 Hz, in the aft direction near the maximum radiation angle range, there is a nonlinear loss of level for all three engine conditions. In the forward direction, however, note that there is an increase in ν_N ; this appears to be caused by nonlinear difference-frequency generation in a spatial region where the peak frequency is 400-600 Hz. In considering the three maps, note that the magnitudes of the nonlinear changes increase with engine condition.

At 10 kHz in Fig. 2, ν_N is generally greatest along the angles of maximum radiation for each engine condition, but is slightly skewed toward the forward direction, likely because of increasing peak frequency for similar sound levels. At 50% ETR, nonlinearity is confined to a relatively narrow angular range, but even this is small, ≤ 0.06 dB/m. At 75% and 130% ETR, the nonlinearity is significantly greater, and, as expected, grows with engine power. At afterburner, the range over which nonlinearity is present grows in that $\nu_N \geq 0.1$ dB/m for all angles and nearly all distances.

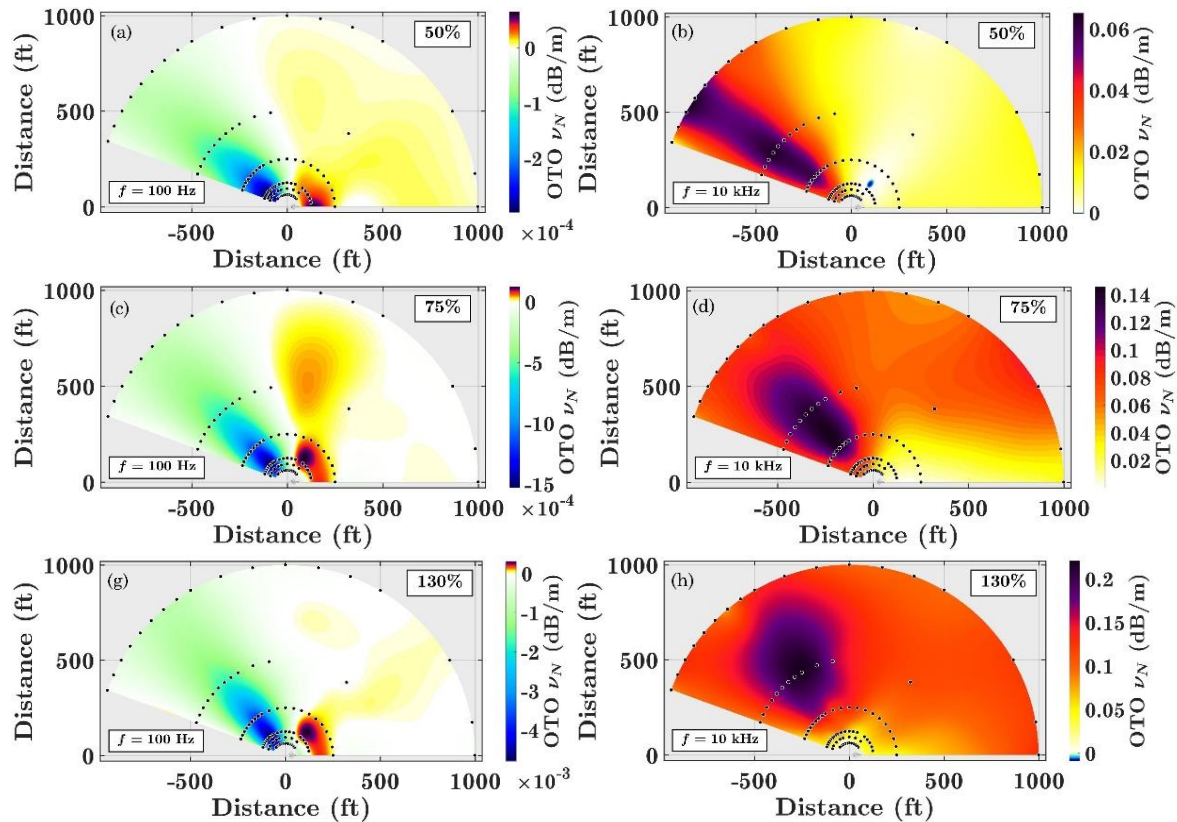


Figure 2. v_N at the 100 Hz and 10 kHz OTO bands, averaged across four run-ups at 130% ETR.

Although nonlinearity at 10 kHz increases both in magnitude and angular aperture, the question of nonlinear significance needs to be jointly considered with v_S and v_α . First, v_S varies from -0.9 to -0.06 dB/m over the propagation range. Thus, geometric spreading is the dominant effect close to the source, but at 305 m, spreading's local rate of change can be smaller than that of nonlinearity. At 100 Hz, $v_\alpha \approx -3e-4$ dB/m, and at 10 kHz, $v_\alpha \approx -0.18$ dB/m, with these values varying slightly with changes in atmospheric conditions. Figure 3 shows $v_\alpha + v_N$ at 10 kHz for 50%, 75%, and 150% ETR, with all three maps on a common color scale. At 50% ETR, $v_\alpha \gg v_N$ over much of the angular range, but the net attenuation rate is less than linear absorption, only about -0.1 dB/m, at far aft angles. Propagation modeling by Reichman *et al.*¹³ shows, in fact, a slower measured decay of high frequencies at 150°. At 75% ETR, linear absorption accounts for the losses directly in front of the aircraft, but nonlinearity reduces the apparent atmospheric absorption rate at most angles by at least half. Finally, the combined effect of nonlinearity and linear absorption at 130% ETR is similar at most angles is only slightly less than the maximum at 75% ETR. It is curious that at 152 m (500 ft), the microphones between 110° and 135° show $v_\alpha + v_N > 0$. Although theory^{3,11} indicates $v_\alpha + v_N$ should be negative after shocks form and in the old-age region, the positive sum at six adjacent microphones suggests a physical propagation effect and not anomalous scattering or reflections. This hypothesis is strengthened by examination of the time-domain average steepening factor for 130% ETR. The average steepening factor,¹⁴ as its name connotes, characterizes the average slopes within the waveform. Along the angles containing these six microphones, the average steepening increases from 19 to 76 m, lessens between 76 and 152 m, and then increases again between 152 and 305 m. This suggests that the positive $v_\alpha + v_N$ is the result of some propagation phenomenon. One likely cause is local meteorology, but another possible contributing factor is the <1 m tall sagebrush that is scattered between 76 and 152 m, but that is more dense¹² between 80 and 120 m and 105° and 125°. While the shrubs are far too short to impede line-of-sight propagation between aircraft and microphone, they may have altered ground reflections and the slightly noncollinear nonlinear propagation and/or contributed to temperature and wind variations in the vicinity.

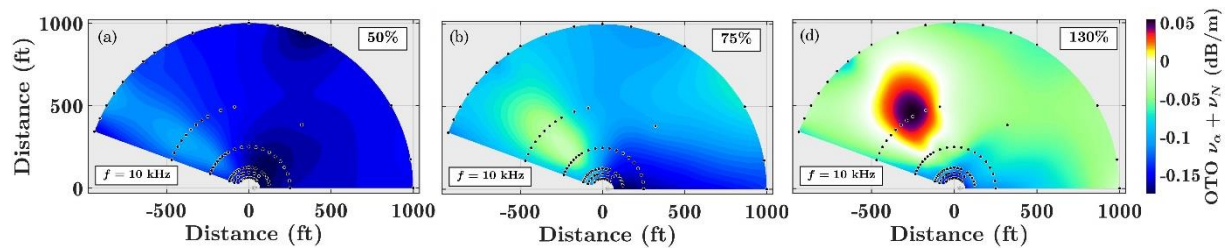


Figure 3. $v_{\alpha} + v_N$ at 10 kHz for 50%, 75% and 150% ETR.

4. CONCLUSION

This paper has described a quantitative analysis of the relative importance of frequency-dependent nonlinearity and absorption in noise radiation from the F-35A. Near the peak-frequency region of the spectrum, the spatial rate of change due to nonlinearity is slightly negative, whereas at high frequencies, it is of greater magnitude and positive. At high engine powers, the combined effect of absorption and nonlinearity results in a slight net loss of high-frequency spectral levels beyond geometric spreading.

ACKNOWLEDGMENTS

This work was funded in part by a Phase I SBIR sponsored by the Air Force Research Laboratory. Data courtesy of the F-35 Joint Program office. (Distribution A - Approved for Public Release; Distribution is Unlimited. Cleared 6/28/18; JSF18-643.)

REFERENCES

- ¹K. L. Gee, V. W. Sparrow, M. M. James, J. M. Downing, C. M. Hobbs, T. B. Gabrielson and A. A. Atchley, "The role of nonlinear effects in the propagation of noise from high-power jet aircraft," *J. Acoust. Soc. Am.* **123**, 4082-4093 (2008).
- ²K. L. Gee, T. B. Neilsen, A. T. Wall, J. M. Downing, M. M. James, and R. L. McKinley, "Propagation of crackle-containing jet noise from high-performance engines", *Noise Control Eng. J.* **64**, 1–12 (2016).
- ³B. O. Reichman, K. L. Gee, T. B. Neilsen and K. G. Miller, "Quantitative analysis of a frequency-domain nonlinearity indicator," *J. Acoust. Soc. Am.* **139**, 2505-2513 (2016).
- ⁴K. G. Miller and K. L. Gee, "Model-scale jet noise analysis with a single-point, frequency-domain nonlinearity indicator," *J. Acoust. Soc. Am.* **143**, 3479–3492 (2018).
- ⁵C. L. Morfey and G. P. Howell, "Nonlinear propagation of aircraft noise in the atmosphere," *AIAA J.* **19**, 986-992 (1981).
- ⁶K. L. Gee, T. B. Gabrielson, A. A. Atchley and V. W. Sparrow, "Preliminary Analysis of Nonlinearity in Military Jet Aircraft Noise Propagation," *AIAA J.* **43**, 1398-1401 (2005).
- ⁷S. McInerny, K. L. Gee, M. Downing and M. James, "Acoustical nonlinearities in aircraft flyover data," *AIAA Paper* 2007-3654 (2007).
- ⁸B. P. Petitjean, K. Viswanathan and D. K. McLaughlin, "Acoustic pressure waveforms measured in high speed jet noise experiencing nonlinear propagation," *Int. J. Aeroacoust.* **5**, 193-215 (2006).
- ⁹L. E. Falco, "Single-point nonlinearity indicators for the propagation of high amplitude acoustic signals," PhD Thesis, The Pennsylvania State University, (2007).
- ¹⁰S. A. McInerny and S. M. Ölçmen, "High-intensity rocket noise: Nonlinear propagation, atmospheric absorption, and characterization," *J. Acoust. Soc. Am.* **117**, 578-591 (2005).
- ¹¹K. G. Miller, K. L. Gee and B. O. Reichman, "Asymptotic behavior of a frequency-domain nonlinearity indicator for solutions to the generalized Burgers equation," *J. Acoust. Soc. Am.* **140**, EL522-EL527 (2016).
- ¹²M. M. James, A. R. Salton, J. M. Downing, K. L. Gee, T. B. Neilsen, B. O. Reichman, R. McKinley, A. T. Wall and H. Gallagher, "Acoustic Emissions from F-35 Aircraft during Ground Run-Up," *AIAA paper no.* 2015-2375 (2015).
- ¹³B. O. Reichman, A. T. Wall, K. L. Gee, T. B. Neilsen, J. M. Downing, M. M. James and R. L. McKinley, "Modeling Far-field Acoustical Nonlinearity from F-35 Aircraft during Ground Run-up," *AIAA Paper* 2016-1888, (2016).
- ¹⁴M. B. Muhlestein, K. L. Gee, T. B. Neilsen and D. C. Thomas, "Evolution of the average steepening factor for nonlinearly propagating waves," *J. Acoust. Soc. Am.* **137**, 640-650 (2015).